CHAPTER 1
Introduction
CHAPTER 2
Machining Dynamics
CHAPTER 3
Robust Control Approach
CHAPTER 4
Hardware-in-the-Loop Test System for Machining Emulation
CHAPTER 5
Structural Dynamics: Modelling and Identification

CHAPTER 6

Optimized Controller Designs

6.1 Introduction

This chapter will present the detailed design of the optimized controllers for the experimental system. The necessary theory for the controller formulations and synthesis problems was given in Chapter 3. The system models that will be used to synthesize the controllers were also obtained in suitable form in Chapter 5. Two versions of the model with different values for the system matrices were obtained, as defined by (5.14) for the FE model and (5.20) for the system ID model. For all cases, the general form for the system state space model is

$$\begin{aligned} \dot{x} &= Ax + B_u u + B_w w \\ y_t &= C_t x \\ y_m &= C_m x. \end{aligned} \tag{6.1}$$

6.1.1 Stability boundary in cutting process with control feedback

As some of the controller designs in this thesis involve time-delayed feedback, basic calculation of the cutting stability boundary, as given by (2.9) and (2.10) is not appropriate (if there are multiple time-delayed feedback loops as for the general time-delay system model). The time-delayed feedback structure for active control scheme is shown in Figure 6.1. The controller input is the set of measured variables y_m as already described in Section 3.1.4. Active control is achieved by a linear dynamic feedback that depends on the time-delay τ. In practice, τ would be known from the measured rotational speed and so such a controller can always be implemented. A general Laplace domain representation of the feedback control law has the form $U(s) = H_c(s,\tau)Y_m(s)$ and the closed-loop transfer function from cutting force w to the tool deflection y_t is

$$G(s,\tau) = C_t \left(sI - A - B_u H_c(s,\tau) \right)^{-1} B_w . \tag{6.2}$$

Combining $Y_t(s) = G(s,\tau)W(s,\tau)$ with the Laplace domain version of the cutting force in (2.5) we obtain the transfer function from the zero-vibration mean chip thickness h_m to the cutting tool displacement vibration y_t as $T_{yh}(s,\tau) = Y_t(s) / H_m(s)$, for which

$$T_{yh}(s,\tau) = \frac{b_K G(s,\tau)}{1 + b_K G(s,\tau)\left(1 - e^{-\tau s}\right)} . \tag{6.3}$$

In order to predict the cutting stability for the time-delay system with implementation of a delay-dependent control feedback, a numerical optimization must be used to find unstable solutions based on the transfer function (6.3). The problem then is to determine the solution to the characteristic equation with $s = \mathrm{j}\omega_c$. Thus, the conditions are

(i) $1 + b_K \operatorname{Re}\left(G(\mathrm{j}\omega_c, \tau)(1 - e^{-\tau \mathrm{j}\omega_c}) \right) = 0$

(ii) $\operatorname{Im}\left(G(\mathrm{j}\omega_c, \tau)(1 - e^{-\tau \mathrm{j}\omega_c}) \right) = 0$

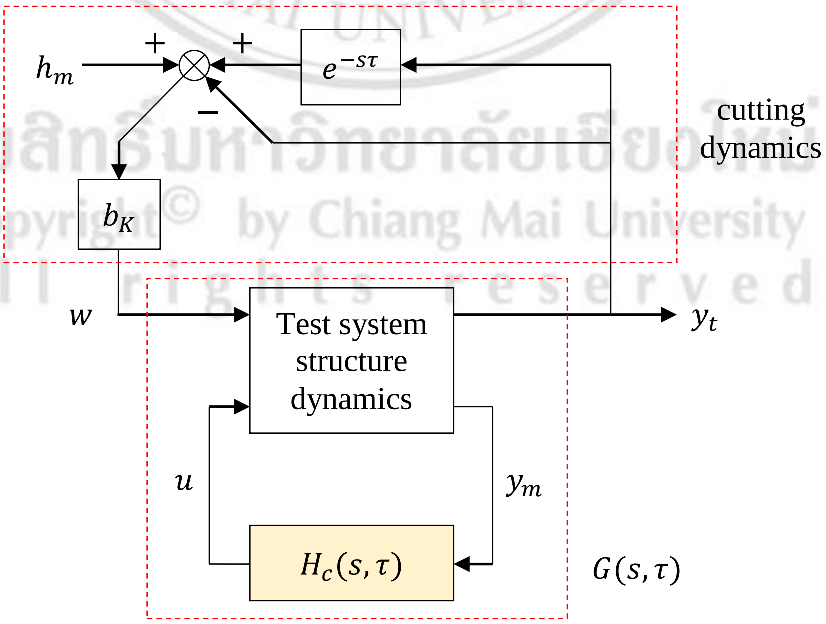

Figure 6.1 The time-delayed feedback structure for active control

From (i) and (ii) we obtain, as before

$$b_{K,\max}(\tau) = \frac{-1}{\min\limits_{\omega_c}\left(\mathrm{Re}\left(G_\tau(\omega_c,\tau)\big|_{\mathrm{Im}\left(G_\tau(\omega_c,\tau)\right)=0}\right)\right)} > 0 \qquad (6.4)$$

where $G_\tau(\omega_c,\tau) = G(\mathrm{j}\omega_c,\tau)\left(1-e^{-\tau \mathrm{j}\omega_c}\right)$. A stability lobe diagram may be constructed as follows:

1. Choose a rotational speed Ω and set $\tau = 2\pi / N_t\Omega$.
2. Numerically find all zeros of $\mathrm{Im}\left(G_\tau(\omega_c,\tau)\right)$ over an interval $\omega_c \in \left[\omega_{c1},\omega_{c2}\right]$ condition (ii).
3. For the solutions from step 2, find $g = \min\left(\mathrm{Re}\left(G_\tau(\omega_c,\tau)\right)\right)\big|_{\mathrm{Im}(G_\tau)=0} < 0$.
4. The stability limit is given by $b_K = -1/g$ (condition (i)) and can be plotted against Ω.
5. Choose the new spindle speed and return to step 1. The rotational speed is varied within a range of values of interest $\Omega \in \left[\Omega_1,\Omega_2\right]$.

6.1.2 Model errors for controller synthesis

This section presents the evaluation of model error results for the test system model, as required for robust control synthesis. As we consider two main types of controller design, which are state feedback controller and output feedback controller, the model error definition must be different for each controller type and is described in the following.

The absolute additive error in the test system model Δ_a was already defined in Chapter 3, (3.3):

$$\Delta_a(s) = G^{act}(s) - G^m(s).$$

The additive error can be established from the frequency response matrices $G^{act}(\mathrm{j}\omega)$, as measured from the test system, and $G^{m}(\mathrm{j}\omega)$ for the identified model (5.14). Note that for these models the input signal is the control force (u):

$$G^{act}(\mathrm{j}\omega) = \begin{bmatrix} g_{y_a u} \\ g_{y_t u} \\ {}_v g_{y_a u} \\ {}_v g_{y_t u} \end{bmatrix} \text{ and } G^{m}(\mathrm{j}\omega) = \left(\mathrm{j}\omega I - A\right)^{-1} B_u \tag{6.5}$$

where $G^{act}(\mathrm{j}\omega)$ is defined pointwise over ω for test frequencies used in the experimental frequency response measurements. Using these values, we may construct the difference error compared with the system ID model, which we define as

$$\Delta_a = \begin{bmatrix} \delta_1 \\ \delta_2 \\ \delta_{v1} \\ \delta_{v2} \end{bmatrix}.$$

The additive error results are shown in Figure 6.2. We can see that the errors $(\delta_1 \text{ and } \delta_2)$ for the displacement outputs looks smaller than that for the velocity outputs $(\delta_{v1} \text{ and } \delta_{v2})$. This is because the velocities are not directly measured values but are obtained by real-time differentiation of the displacement signals.

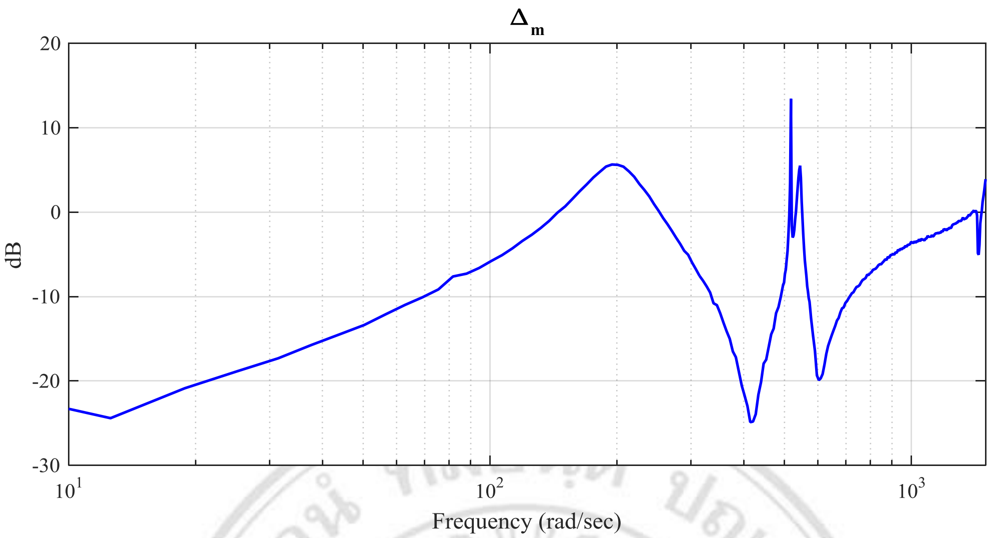

Figure 6.3 Multiplicative uncertainty for displacement output model

We now focus on the input multiplicative error $\Delta_m^{in} = \Delta_m$. For state feedback control, the effective multiplicative error is not independent of the controller H_c (see Section 3.1.4 in (3.7)) and in this case $\Delta_m = H_c\Delta_a\left(I - H_c\Delta_a\right)^{-1}$. For output feedback control law the plant becomes square (SISO) and so Δ_m can be calculated from Δ_a as in (3.4). The results are shown in Figure 6.3. We can see that there are certain frequencies where the error is large and these potentially can limit the synthesized controller gain

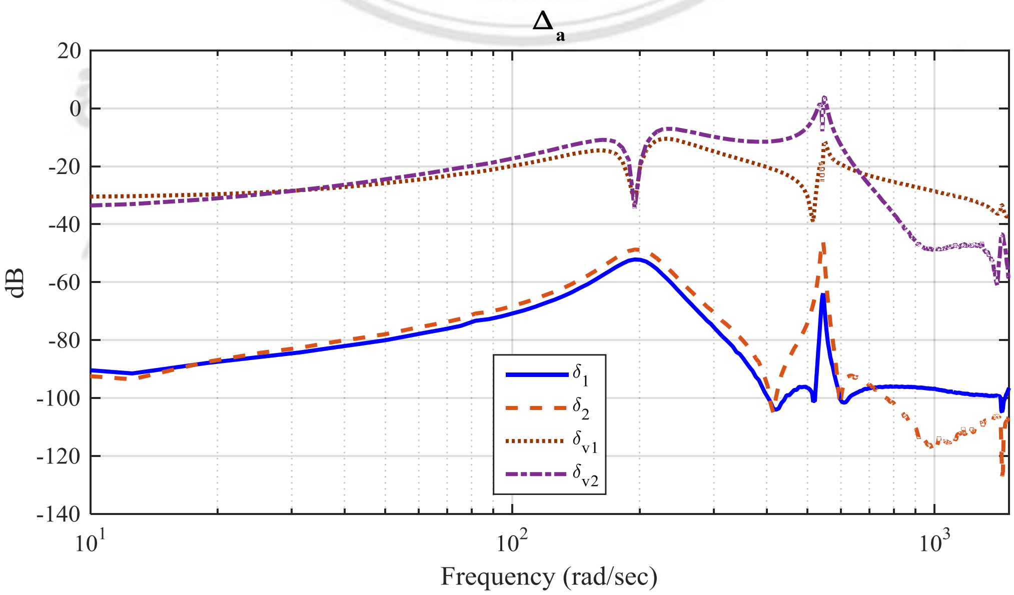

Figure 6.2 Additive error for state output model

and performance.

Weighting function determination

To determine the required weighting function (W_r), the multiplicative uncertainty must first be estimated and then $W_r(s)$ chosen as a stable bounding transfer function, as described in Section 3.1.4. Accordingly

$$\left|\Delta_m(j\omega)\right| < \left|W_r(j\omega)\right| .$$

For the case studies in this chapter, the weighting function is chosen as a second order $s-$domain transfer function in the form

$$W_r(s) = K_w \frac{s^2 + \varsigma_1\omega_1 s + \omega_1^2}{s^2 + \varsigma_2\omega_2 s + \omega_2^2} \tag{6.6}$$

where, the designed values of ς_1, ς_2, ω_1 and ω_2 are chosen according to the anticipated multiplicative error, as shown in Figure 6.3, and K_w is an overall scaling factor. A state space realization of (6.6) may also be readily obtained for inclusion in the augmented plant definition, as in (3.9).

$$\begin{aligned} \dot{x}_r &= A_r x_r + B_r u \\ \tilde{u} &= K_w\left(C_r x_r + D_r u\right). \end{aligned} \tag{6.7}$$

6.1.3 Problem formulation and the augmented system

The augmented plant, as defined for specification of the robust stability/performance objectives for the controller design is shown in Figure 6.4. The weighted output that will be used for the robust stability criterion is $\tilde{u}$. The robust stability criterion with respect to multiplicative errors in the plant model is in the form of an H_∞ norm-bound:

$$\left\|W_r T_{ud}\right\|_\infty < 1 \tag{6.8}$$

where the complementary sensitivity function T_{ud} is the closed-loop transfer function from d to u and W_r is the multiplicative error-bound. Alternatively, we can seek to maximize robustness for a given overall form of uncertainty (given shape of $W_r(j\omega)$) by imposing

$$\|W_r T_{ud}\|_\infty < \gamma \tag{6.9}$$

and then minimizing the value of γ in the synthesis routine.

Note that, the particular type of optimization used (Equation (6.8) or (6.9)) will depend on the controller design approach. For (6.8) the value of K_w must be set appropriately prior to synthesis, whereas for (6.9) the initial value of K_w is not critical.

The system model to use for synthesizing the controller combines the test system structure model (6.1) and the weighting function model with the exogenous perturbation input d adding to u as follows:

$$\begin{aligned} \dot{\tilde{x}} &= \tilde{A}\tilde{x} + \tilde{B}_d d + \tilde{B}_w w + \tilde{B}_u u \\ \tilde{u} &= K_w\left(\tilde{C}_r\tilde{x} + \tilde{D}_r u\right) \\ y_t &= \tilde{C}_t\tilde{x} \\ y_m &= \tilde{C}_m\tilde{x} \end{aligned} \tag{6.10}$$

where $\tilde{A} = \begin{bmatrix} A & 0 \\ 0 & A_r \end{bmatrix}$, $\tilde{B}_d = \begin{bmatrix} B_u \\ 0 \end{bmatrix}$, $\tilde{B}_w = \begin{bmatrix} B_w \\ 0 \end{bmatrix}$, $\tilde{B}_u = \begin{bmatrix} B_u \\ B_r \end{bmatrix}$, $\tilde{C}_m = \begin{bmatrix} C_m & 0 \end{bmatrix}$, $\tilde{C}_t = \begin{bmatrix} C_t & 0 \end{bmatrix}$,

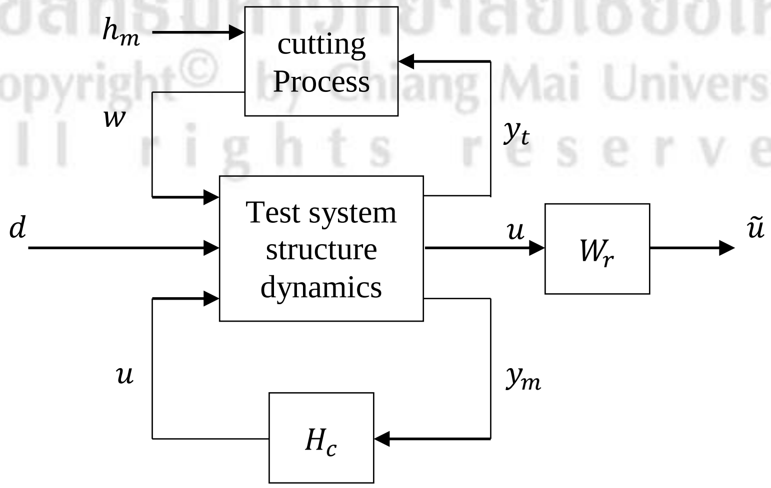

Figure 6.4 Augmented system structure for robust control

$\tilde{C}_r = \begin{bmatrix} 0 & C_r \end{bmatrix}$, $\tilde{D}_r = D_r$ and the augment state vector $\tilde{x} = \begin{bmatrix} x \\ x_r \end{bmatrix}$. Next, considering the cutting force model (2.4) gives

$$w = b_K \left(h_m + \tilde{C}_t \tilde{x}(t-\tau) - \tilde{C}_t \tilde{x} \right),$$

which can be combined with (6.10), leading to the augmented time-delay system model

$$\begin{array}{rcl} \dot{\tilde{x}} & = & \tilde{A}_0 \tilde{x} + \tilde{A}_\tau \tilde{x}(t-\tau) + \tilde{B}_d d + \tilde{B}_w w_0 + \tilde{B}_u u \\ \tilde{u} & = & K_w \left(\tilde{C}_r \tilde{x} + \tilde{D}_r u \right) \\ y_t & = & \tilde{C}_t \tilde{x} \\ y_m & = & \tilde{C}_m \tilde{x} \end{array} \tag{6.11}$$

where $\tilde{A}_0 = \tilde{A} - b_K \tilde{B}_w \tilde{C}_t$, $\tilde{A}_\tau = b_K \tilde{B}_w \tilde{C}_t$.

6.2 State Feedback Controllers

Considering the augmented system in (6.10) with full state measurement $y_m = \tilde{x}$, (implying $C_m = I$), this section presents the design synthesis for a state feedback control law in the form

$$u = K_0 \tilde{x} + K_\tau \tilde{x}(t-\tau) = K_0 y_m + K_\tau y_m(t-\tau) \tag{6.12}$$

where state feedback gains K_0 and K_τ are to be determined. The controlled system is given by

$$\begin{array}{rcl} \dot{\tilde{x}} & = & \left(\tilde{A}_0 + \tilde{B}_u K_0 \right) \tilde{x} + \left(\tilde{A}_\tau + \tilde{B}_u K_\tau \right) \tilde{x}(t-\tau) + \tilde{B}_d d + \tilde{B}_w w_0 \\ \tilde{u} & = & \left(\tilde{C}_r + \tilde{D}_r \tilde{B}_u K_0 \right) \tilde{x} + \tilde{D}_r \tilde{B}_u K_\tau \tilde{x}(t-\tau) \\ y_t & = & \tilde{C}_t \tilde{x}. \end{array} \tag{6.13}$$

To ensure that the system (6.13) satisfies the H_∞ norm-bounded criterion in (6.9), the following equivalent condition is considered

$$\|\tilde{u}\|_{L_2} \le \gamma \|d\|_{L_2}, \ \forall d \in L_2[0, \infty).$$

The method of controller synthesis based on the LMI formulation with LKF follows the theory in Section 3.1.4. The details are now given:

6.2.1 LMI formulation for state feedback synthesis

If there exist positive definite matrix $L > 0, S > 0$ and matrices K_0^* and K_τ^* such that the following LMI holds:

$$\Psi^* = \begin{bmatrix} \tilde{A}_0 L + L\tilde{A}_0^T + \tilde{B}_u K_0^* + K_0^{*T}\tilde{B}_u^T + S & \tilde{A}_\tau L + \tilde{B}_u K_\tau^* & \tilde{B}_d & L\tilde{C}_r^T + K_0^{*T}\tilde{D}_r^T \\ & -S & 0 & K_\tau^{*T}\tilde{D}_r^T \\ & & -\gamma I & 0 \\ sym & & & -\gamma I \end{bmatrix} < 0 \qquad (6.14)$$

where $L = P^{-1}$, $S = L^T Q L$, $K_0^* = K_0 L$ and $K_\tau^* = K_\tau L$ then, the time-delay system with controller in (6.10) is stable and the H_∞ norm from the d to $\tilde{u}$ is less than γ.

An optimized solution to (6.14) can be obtained via a generalized eigenvalue problem (GEVP) defined as

$$\begin{aligned} &\text{Minimize } \gamma \text{ over } L, S, X, K_0^*, K_\tau^* \\ &\text{subject to } L > 0, S > 0, X > 0 \\ &\Psi_X^* < 0 \\ &X > \gamma I \end{aligned} \qquad (6.15)$$

where

$$\Psi_X^* = \begin{bmatrix} \tilde{A}_0 L + L\tilde{A}_0^T + \tilde{B}_u K_0^* + K_0^{*T}\tilde{B}_u^T + S & \tilde{A}_\tau L + \tilde{B}_u K_\tau^* & \tilde{B}_d & L\tilde{C}_r^T + K_0^{*T}\tilde{D}_r^T \\ & -S & 0 & K_\tau^{*T}\tilde{D}_r^T \\ & & -X & 0 \\ sym & & & -X \end{bmatrix} < 0 . \qquad \square$$

We can also design some different versions of the state feedback controllers in order to compare the effect of the delayed state feedback on cutting stability. The three design versions considered in this study are as follows:

LKF-SFC1

For feedback of current state values only, the control law can be written as

$$u = K\tilde{x}$$

LKF-SFC2

Control with feedback of current and time-delayed state values with optimization as already described in Section 6.2

$$u = K_0\tilde{x} + K_\tau\tilde{x}(t-\tau)$$

LKF-SFC3

A two-step optimization of gain values for current and time-delayed states in which the time-delayed state gains are optimized and the current state feedback gains are those from LKF-SFC1.

6.2.2 Linear quadratic regulator design (LQR-SFC)

For comparison, an optimal Linear Quadratic Regulator (LQR) controller design is also introduced here. Note that LQR controller design has been applied previously for chatter control e.g. in [30], [37]. Here we consider a quadratic regulator having similar robustness properties to the previous designs, in terms of the treatment of model uncertainty. In this case, however, the design is based on the linear delay-free model with $b_K = 0$, i.e. without any direct account of the cutting model. Instead, we seek a controller that minimizes the H_2 norm from w to y_t subject to the robustness constraint $\|T_{\tilde{u}d}\|_\infty < \gamma$. To this end we seek a solution $V(\tilde{x}) = \tilde{x}^T P \tilde{x}$ satisfying

$$\begin{aligned} \dot{V}(\tilde{x}) + \beta\left(\tilde{u}^T\tilde{u} - d^T d\right) + y_t^T y_t &\leq 0 \\ V\left(\tilde{B}_w\right) &< \alpha^2 \end{aligned} \qquad (6.16)$$

for some $\beta > 0$. By standard arguments [43], the system is then stable for all $\|d\|_{L_2} \leq \|\tilde{u}\|_{L_2}$ and the H_2 norm from w to y_t is less than α. The state-feedback synthesis problem can be cast as a standard LMI problem involving minimization of α subject to (6.16). The derivation of the LMI equations follows a similar procedure to that in Section 3.1.4.

6.3 Output Feedback Controllers

6.3.1 Optimized designs based on previous techniques

Three controller design cases are considered based on using different concepts to account for the cutting force effects. These techniques have been used in previous studies and are referred to as OFC 1-3.

OFC1: Dynamics compliance minimization

The *dynamic compliance minimization* approach was introduced by previous researchers and used in optimal controller design for AMB milling spindles, e.g. as in [31]. For this approach, the cutting force equation is not included specifically as part of the system model, which is shown in Figure 6.5. The inputs d and output u are included for the robustness specification as before, with the weighting function chosen according to the multiplicative error. An additional design constraint for this control approach is for the cutting stability which can be specified by

$$\left\| T_{y_t w} \right\|_\infty < \beta . \quad (6.17)$$

This criterion ensures that $\mathrm{Re}\left(T_{y_t w}\right) < \beta$ and, hence, according to (2.9), we also can conclude that $b_{k,\max} > \dfrac{1}{2\beta}$. The H_∞ norm-bound constraint (6.17) can be treated via the standard dissipation inequality (Theorem 3.5):

$$\dot{V} + \frac{1}{\beta} y_t^T y_t - \beta w^T w \le 0 \quad (6.18)$$

which leads to the LMI constraint, as in Section 3.4.2:

$$\Psi_{C1} = \begin{bmatrix} PA_{cl} + A_{cl}^T P & PB_{cl,w} & C_{cl,t}^T \\ & -\beta I & \\ sym & & -\beta I \end{bmatrix} < 0 . \quad (6.19)$$

Both stability constraints,

$$\left\| T_{y_t w} \right\|_\infty < \beta$$
$$\left\| T_{\tilde{u} d} \right\|_\infty < 1$$

must be treated simultaneously and so a two-channel LMI formulation is appropriate, where a single quadratic Lyapunov function is used to establish both constraints via simultaneous solution of two LMIs: $\Psi_0 < 0$ and $\Psi_{C1} < 0$. For the minimization problem for this case, we can set $\gamma = 1$ (for given value of K_w) and then the minimize the value of β within the optimization routine. Next, the controller matrices are obtained as described in Section 3.4.2.

OFC2: Norm-Bound treatment of delay

In order to better describe the cutting dynamics we may instead account for the time-delay effect by a norm-bound constraint as previously considered in [28], [32]. In this case, the time-delay block in the cutting force model is omitted, as shown in Figure 6.6. The cutting force equation can then be written in the form:

$$w(t) = b_K \left(q(t) - y_t(t) \right) \tag{6.20}$$

where $q(t) = y_t(t-\tau)$. Or, in the Laplace domain $Q(s) = e^{-s\tau} Y_t(s)$. Hence, the time delay transfer function may be treated as an external uncertainty $\Delta_\tau(s) = e^{-s\tau}$. It is easy to show that $\left\| \Delta_\tau \right\|_\infty \leq 1$. Hence, the specification for stability during cutting follows from

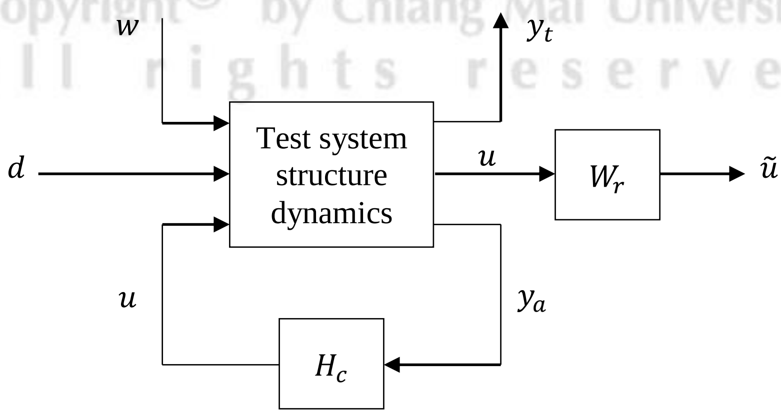

Figure 6.5 System plant for dynamics compliance minimization

the small gain theorem [43] applied to the closed-loop system, where the effects of $\Delta_\tau(s)$ are treated via the exogenous input q:

$$\left\| T_{y_t q} \right\|_\infty < 1. \tag{6.21}$$

This H_∞ norm-bound constraint can again be treated via the standard dissipation inequality (Theorem 3.5):

$$\dot{V} + y_t^T y_t - q^T q \leq 0. \tag{6.22}$$

So that, the LMI form for this case can be defined as

$$\Psi_{C2} = \begin{bmatrix} PA_{cl} + A_{cl}^T P & PB_{cl,w}^{b_K} & C_{cl,t}^T \\ & -I & \\ sym & & -I \end{bmatrix} < 0. \tag{6.23}$$

Again there are two design constraints

$$\begin{aligned} \left\| T_{\tilde{u}d} \right\|_\infty &< \gamma \\ \left\| T_{y_t q} \right\|_\infty &< 1 \end{aligned}$$

which must be treated simultaneously via a two-channel LMI formulation. A single quadratic Lyapunov function is used to establish both constraints via simultaneous solution of the two LMIs: $\Psi_0 < 0$ and $\Psi_{C1} < 0$. For the minimization problem in this

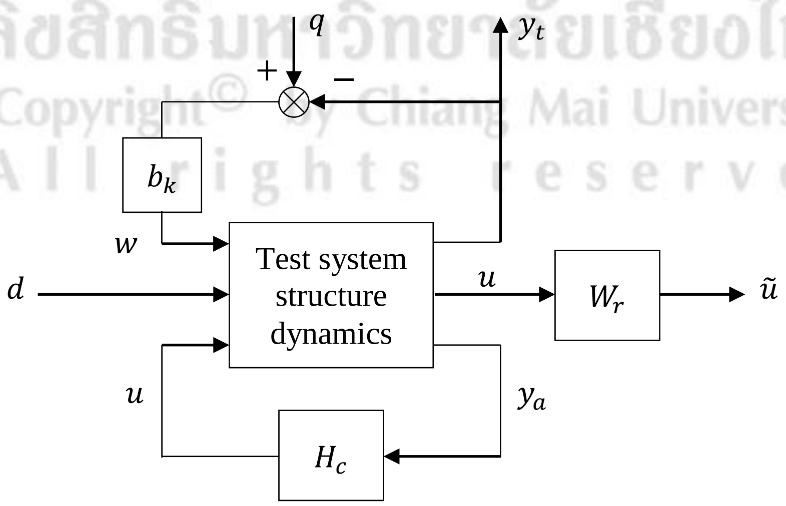

Figure 6.6 System plant for norm-bound treatment of delay

case, we can minimize γ for a given value of b_K (which is embedded in the LMIs).

OFC3: Padé approximation of delay

A Padé approximation of time delay effects has been considered previously for chatter prediction and control in a number of studies [20], [21], [28]. In this case, the time-delay in the cutting force model is treated by using a Padé approximation in the form $E_\tau(s) \approx e^{-s\tau}$. The system plant is shown in Figure 6.7. Thus the cutting force can be written

$$W(s) = b_K\left(H_m(s) + \left(E_\tau(s) - 1\right)Y_t(s)\right). \tag{6.24}$$

The Padé approximation has the presented form in (2.12) which can be realized in the state space form

$$\begin{aligned} \dot{x}_P &= A_P x_P + B_P y_t \\ y_{t,\tau} &= C_P x_P + D_P y_t. \end{aligned} \tag{6.25}$$

Firstly, we have to combine the system model in (6.1) and (6.25) to obtain the linear system with time-delay approximation. This yields

$$\begin{aligned} \dot{\varpi} &= A_\varpi \varpi + B_{\varpi,d} d + B_{\varpi,w} w_0 + B_{\varpi,u} u \\ y_t &= C_{\varpi,t} \varpi \\ y_a &= C_{\varpi,a} \varpi \end{aligned} \tag{6.26}$$

where $A_\varpi = \begin{bmatrix} A + b_K B_w \left(D_P - 1\right) C_t & b_K B_w C_P \\ B_P C_t & A_P \end{bmatrix}$, $B_{\varpi,d} = \begin{bmatrix} B_u \\ 0 \end{bmatrix}$, $B_{\varpi,w} = \begin{bmatrix} B_w \\ 0 \end{bmatrix}$, $B_{\varpi,u} = \begin{bmatrix} B_u \\ 0 \end{bmatrix}$,

$C_{\varpi,a} = \begin{bmatrix} C_a & 0 \end{bmatrix}$, $C_{\varpi,t} = \begin{bmatrix} C_t & 0 \end{bmatrix}$ and the state vector for the system is $\varpi = \begin{bmatrix} x \\ x_P \end{bmatrix}$.

In this case a one channel LMI optimization for $\Psi_0 < 0$ can be used to obtain the controller solution satisfying

$$\left\| T_{\tilde{u}d} \right\|_\infty < \gamma.$$

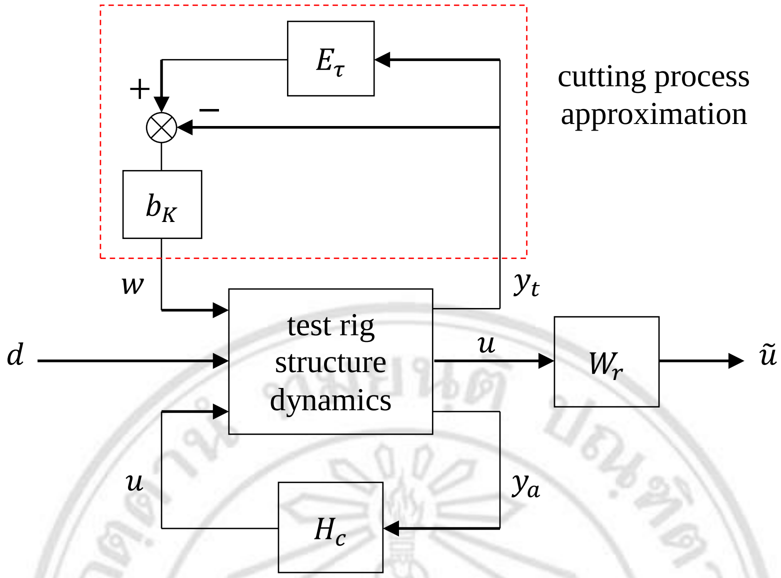

Figure 6.7 System plant for Padé approximation of delay

6.3.2 Optimized designs based on LKF approach

Considering, again, the augment system in (6.11) with measured output being $y_m = y_a$. The output feedback control law with time-delayed feedback has the form

$$\begin{aligned} \dot{x}_K &= A_K x_K + A_{K\tau} x_K(t-\tau) + B_K y_a + B_{K\tau} y_a(t-\tau) \\ u &= C_K x_K + C_{K\tau} x_K(t-\tau) + D_K y_a + D_{K\tau} y_a(t-\tau) \end{aligned} \quad (6.27)$$

where controller matrices A_K, $A_{K\tau}$, B_K, $B_{K\tau}$, C_K, $C_{K\tau}$, D_K, $D_{K\tau}$ are to be determined. The closed-loop system is given by

$$
\begin{aligned}
\dot{x}_{cl} &= A_{cl,0}x_{cl} + A_{cl,\tau}x_{cl}(t-\tau) + B_{cl,d}d + B_{cl,w}w_0 \\
\tilde{u} &= C_{cl,r}x_{cl} + C_{cl,r\tau}x_{cl}(t-\tau) \\
y_t &= C_{cl,t}x_{cl}
\end{aligned}
\tag{6.28}
$$

where

$$
A_{cl,0} = \begin{bmatrix} \tilde{A}_0 + \tilde{B}_u D_K \tilde{C}_a & \tilde{B}_u C_K \\ B_K \tilde{C}_a & A_K \end{bmatrix}, \qquad A_{cl,\tau} = \begin{bmatrix} \tilde{A}_\tau + \tilde{B}_u D_{K\tau} \tilde{C}_a & \tilde{B}_u C_{K\tau} \\ B_{K\tau} \tilde{C}_a & A_{K\tau} \end{bmatrix}, \qquad B_{cl,d} = \begin{bmatrix} \tilde{B}_u \\ 0 \end{bmatrix},
$$

$$
B_{cl,w} = \begin{bmatrix} \tilde{B}_w \\ 0 \end{bmatrix}, C_{cl,t} = \begin{bmatrix} \tilde{C}_t & 0 \end{bmatrix}, C_{cl,r} = \begin{bmatrix} \tilde{C}_r + \tilde{D}_r D_K \tilde{C}_a & \tilde{D}_r C_K \end{bmatrix}, C_{cl,r\tau} = \begin{bmatrix} \tilde{D}_r D_{K\tau} \tilde{C}_a & \tilde{D}_r C_{K\tau} \end{bmatrix}
$$

and the state vector of the close-loop system is $x_{cl} = \begin{bmatrix} \tilde{x} \\ x_K \end{bmatrix}$.

To ensure that the system (6.28) satisfies the H_∞ norm-bound criterion in (6.9), the following equivalent condition is considered

$$
\|\tilde{u}\|_{L_2} \le \gamma \|d\|_{L_2}, \ \forall d \in L_2[0,\infty).
$$

The method of controller synthesis based on the LMI formulation with LKF follows the theory in Section 3.4.2. The main steps are as follows:

LMI formulation for output feedback synthesis

If there exist positive matrices $X > 0$, $Y > 0$, $\begin{bmatrix} Q_{11} & Q_{12} \\ sym & Q_{22} \end{bmatrix} > 0$ and the matrices $\hat{A}_K$, $\hat{A}_{K\tau}$, $\hat{B}_K$, $\hat{B}_{K\tau}$, $\hat{C}_K$, $\hat{C}_{K\tau}$, $\hat{D}_K$, $\hat{D}_{K\tau}$ such that the following LMI holds:

$$
\Phi_\Gamma = \begin{bmatrix} \Phi_{11} & \Phi_{12} & \Phi_{13} & \Phi_{14} \\ & \Phi_{22} & 0 & \Phi_{24} \\ & & -\gamma I & 0 \\ sym & & & -\gamma I \end{bmatrix} < 0 \tag{6.29}
$$

where

$$
\Phi_{11} = \begin{bmatrix} \tilde{A}_0 X + X\tilde{A}_0^T + \tilde{B}_u \hat{C}_K + \hat{C}_K^T \tilde{B}_u^T + Q_{11} & \hat{A}_K + \tilde{A}_0 + \tilde{B}_u \hat{D}_K \tilde{C}_a + Q_{12} \\ sym & Y\tilde{A}_0 + \tilde{A}_0^T Y + \hat{B}_K \tilde{C}_a + \tilde{C}_a^T \hat{B}_K^T + Q_{22} \end{bmatrix},
$$

$$\Phi_{12} = \begin{bmatrix} \tilde{A}_\tau X + \tilde{B}_u \widehat{C}_{K\tau} & \tilde{A}_\tau + \tilde{B}_u \widehat{D}_{K\tau} \tilde{C}_a \\ \widehat{A}_{K\tau} & Y\tilde{A}_\tau + \widehat{B}_{K\tau} \tilde{C}_a \end{bmatrix}, \ \Phi_{13} = \begin{bmatrix} \tilde{B}_d \\ Y\tilde{B}_d \end{bmatrix}, \ \Phi_{14} = \begin{bmatrix} X\tilde{C}_r^T + \widehat{C}_K^T \tilde{D}_r^T \\ \tilde{C}_r^T + \tilde{C}_a \widehat{D}_K^T \tilde{D}_r^T \end{bmatrix},$$

$$\Phi_{22} = \begin{bmatrix} Q_{11} & Q_{12} \\ sym & Q_{22} \end{bmatrix} \text{ and } \Phi_{24} = \begin{bmatrix} \widehat{C}_{K\tau}^T \tilde{D}_r^T \\ \tilde{C}_a \widehat{D}_{K\tau}^T \tilde{D}_r^T \end{bmatrix}.$$

Then the time-delay system in (6.28) is stable and the H_∞ norm from d to $\tilde{u}$ less than γ.

The controller matrices can be calculated by a reconstruction from the new variables as follows

$$\begin{aligned}
D_K &= \widehat{D}_K \\
C_K &= \left(\widehat{C}_K - D_K \tilde{C}_a X\right) M^{-T} \\
B_K &= N^{-1}\left(\widehat{B}_K - Y\tilde{B}_u D_K\right) \\
A_K &= N^{-1}\left(\widehat{A}_K - Y\left(\tilde{A}_0 + \tilde{B}_u D_K \tilde{C}_a\right) X - N B_K \tilde{C}_a X - Y\tilde{B}_u C_K M^T\right) M^{-T} \\
D_{K\tau} &= \widehat{D}_{K\tau} \\
C_{K\tau} &= \left(\widehat{C}_{K\tau} - D_{K\tau} \tilde{C}_a X\right) M^{-T} \\
B_{K\tau} &= N^{-1}\left(\widehat{B}_{K\tau} - Y\tilde{B}_u D_{K\tau}\right) \\
A_{K\tau} &= N^{-1}\left(\widehat{A}_{K\tau} - Y\left(\tilde{A}_\tau + \tilde{B}_u D_{K\tau} \tilde{C}_a\right) X - N B_{K\tau} \tilde{C}_a X - Y\tilde{B}_u C_{K\tau} M^T\right) M^{-T}.
\end{aligned}$$

The solution for the unknown matrices of N and M is not unique. However, a suitable method is to use a singular value decomposition based on the constraint equation for the matrices N, M, X and Y which is $YX + NM^T = I$. Therefore,

$$NM^T = I - YX = \left(\Lambda_N \Sigma^{1/2}\right)\left(\Sigma^{1/2} \Lambda_M^T\right)$$

and so we can assign $N = \Lambda_N \Sigma^{1/2}$ and $M^T = \Sigma^{1/2} \Lambda_M^T$.

An optimized solution to (6.29) can be obtained via a generalized eigenvalue problem (GEVP) defined as

$$
\begin{aligned}
&\text{Minimize} \quad \gamma \quad \text{over } X,\ Y,\ Z,\ \begin{bmatrix} Q_{11} & Q_{12} \\ sym & Q_{22} \end{bmatrix} \\
&\qquad \hat{A}_K,\ \hat{B}_K,\ \hat{C}_K,\ \hat{D}_K,\ \hat{A}_{K\tau},\ \hat{B}_{K\tau},\ \hat{C}_{K\tau},\ \hat{D}_{K\tau} \\
&\text{subject to} \quad X > 0,\ Y > 0,\ Z > 0,\ \begin{bmatrix} Q_{11} & Q_{12} \\ sym & Q_{22} \end{bmatrix} > 0 \\
&\qquad \Phi_\Gamma^* < 0 \\
&\qquad Z < \gamma I
\end{aligned}
\tag{6.30}
$$

where

$$
\Phi_\Gamma^* = \begin{bmatrix} \Phi_{11} & \Phi_{12} & \Phi_{13} & \Phi_{14} \\ & \Phi_{22} & 0 & \Phi_{24} \\ & & -Z & 0 \\ sym & & & -Z \end{bmatrix} < 0 .
$$

□